Studying Plasma Electron Temperature in the GOLEM Tokamak

Quentin Potiron* and Matthew Riding†
(Cadarache Winter Event)
(Dated: 15th - 19th February 2021)

In this work, the electron temperature of hydrogen plasma discharges in the GOLEM tokamak (situated in the Czech Technical University, Prague, Czech Republic) was studied experimentally using plasma resistivity estimates inferred from inductive coil diagnostics. The resististivity of the plasma was calculated from the diagnostic measurements and related to plasma electron temperature through the Spitzer theory. The average electron temperature obtained in GOLEM discharges was found to increase with both toroidal magnetic field and plasma current, with the maximum acheived when toroidal magnetic field and plasma current were balanced to give good magneto-hydrodynamic (MHD) stability, and hence long discharge duration. This result is discussed and shown to fit well with theoretical predictions for the behviour of magnetically confined plasmas and the GOLEM device.

I. INTRODUCTION

Applying an external magnetic field to a plasma constrains the motion of both electrons and ions by trapping them into gyrotron orbits around the magnetic field lines[1]. In the tokamak magnetic field configuration, plasma confinement is acheived by circulating magnetic field lines in a toroidal geometry, with the addition of a poloidal magnetic field component to stabilise the plasma against secular drifts. A higher quality of magnetic confinement allows a plasma to acheive a higher temperature in the presence of a heating source, since the confining magnetic field structure restricts the loss of high energy particles to the walls of the vacuum vessel inside which the plasma is contained. Maximising the electron temperature acheivable inside a given device is of great interest to magnetic confinement fusion (MCF) research, as the temperature of an MCF plasma is one of the variables featured in the famous 'fusion triple product' figure of merit for the performance of a fusion plasma[6].

The GOLEM tokamak is a small, ohmically heated device at the Czech Technical University in Prague, Czech Republic. Both the toroidal magnetic field and the inductive toroidal plasma current in GOLEM are generated by the discharge of capacitors, which can be charged to variable voltages[3]. In this work, the charging voltages of these two capacitors were varied across many hydrogen plasma discharges, to investigate the effect of the average toroidal magnetic field strength ($\langle B_T \rangle$) and average toroidal plasma current ($\langle I_P \rangle$) on the average electron temperature ($\langle T_e \rangle$) acheived during a given discharge. Inductive coil diagnostics were used to measure B_T and I_P thoughout individual discharges, and the Spitzer theory of plasma resistivity was used to estimate T_e from I_P and the toroidal loop voltage U_{loop}.

* quentin.potiron@universite-paris-saclay.fr
† matthew.riding@gmail.com

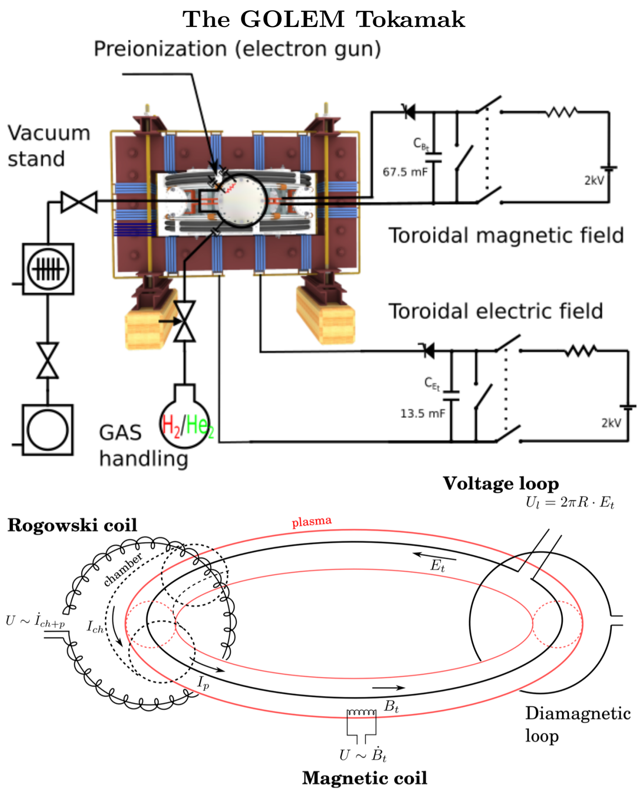

FIG. 1: Top: Diagram of GOLEM tokamak, showing gas handling and main electrical systems (from [3]). Bottom: Illustration of the basic magnetic diagnostics installed on GOLEM (from [6]).

II. DIAGNOSTICS

Figure 1 shows a diagram of the GOLEM tokamak and an illustration of the coil diagnostics used in this work. These diagnostics function on the principle of electromagnetic induction. A loop of wire running poloidally (labelled 'diamagnetic loop' in figure 1) will experience an induced current directly proportional to the rate of change of magnetic flux inside it. Thus by measuring the current induced in this diamagnetic loop over the course of a plasma discharge, a signal is obtained which can be integrated to give B_T as a function of time. The plasma current, I_P, is detected via a Rogowski coil (see figure 1), which is sensitive to the rate of change of the poloidal component of magnetic field, B_θ. The current in this coil can similarly be measured and integrated to give B_θ as a function of time, and this can in turn be related to the amperage of the plasma current flowing toroidally in the tokamak, I_P. Finally, the plasma resistivity can only be estimated if the toroidal loop voltage (or electro-motive force), U_{loop} generated by the tokamak's transformer circuit is also measured alongside the induced plasma current. U_{loop} is measured directly using a toroidal wire.

III. SPITZER THEORY OF PLASMA RESISTIVITY

From measurements of I_P and U_{loop}, an estimate can be made of the paralell resistivity of the plasma ($\eta_{\|}$) produced during any given discharge on GOLEM. 'Parallel' refers to the plasma resistivity when a current is passed paralell to the magnetizing magnetic field lines. This estimate is made according to the Spitzer theory of plasma resistivity[2][5], which gives the following equation for $\eta_{\|}$:

$$\eta_{\|} = \frac{1}{1.96} \frac{4\sqrt{2\pi}}{3} \frac{Z m_e^{1/2} \ln \Lambda}{(4\pi\epsilon_0)^2 (k_B T_e)^{3/2}} \tag{1}$$

It can thus be seen that, given an experimental measurement of $\eta_{\|}$, the electron temperature T_e can be calculated given the atomic number of the plasma ion species (here hydrogen, i.e. $Z = 1$) and an estimate for the Coulomb logarithm $\ln \Lambda$. The data processing system in GOLEM uses a constant value of 17 for this parameter.

IV. EXPERIMENTAL METHODOLOGY

To obtain the dependence of $\langle T_e \rangle$ on $\langle B_T \rangle$ and $\langle I_P \rangle$, a total of 35 discharges were performed, corresponding to seven different values of the toroidal field coil capacitor voltage U_{BT} (from 600V to 1200V in 100V steps), at each of five different values of the current drive transformer capacitor voltage U_{CD} (from 300V to 700V in 100V intervals). Every possible combination of these two capacitor voltages was attempted ($7 \times 5 = 35$), and only one combination failed to breakdown the hydrogen gas to produce a plasma (when U_{BT} was set to its minimum value of 600V, and U_{CD} was set to its maximum value of 700V). For each discharge, all three coil diagnostics described in section II were used to obtain high temporal-resolution profiles of B_T, I_P, U_{loop} and then calculate a profile of T_e via the Spitzer theory described in section III. For each shot, a windowed-averaging method was used to extract the time-averaged quantities $\langle B_T \rangle$, $\langle I_P \rangle$ and $\langle T_e \rangle$.

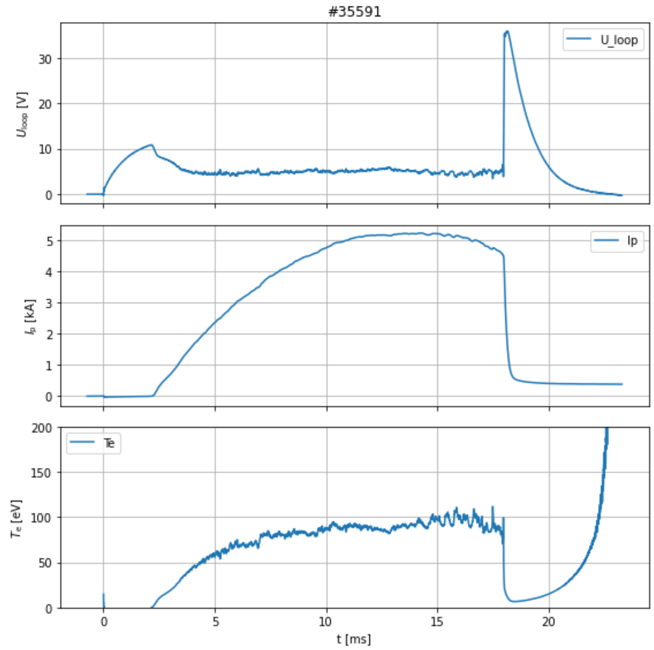

FIG. 2: Time profiles of U_{loop} (top), I_P (middle) and T_e (bottom) from an example discharge ($U_{BT} = 1000$V, $U_{CD} = 400$V). The discharge begins when the plasma breaks down at $t \approx 2.5$ms and ends when the transformer circuit can no longer increase in current, at $t \approx 18$ms. The exact measured discharge duration was 15.71ms.

The mean value of each of these parameters was calculated only over the time range for which they displayed continuous change. Periods with sudden, discontinuous peaks (such as during a period of obvious instability or at the termination of the discharge) were excluded from the calculation of these mean values. In each case, the time window for the calculation of these mean values was adjusted manually.

V. RESULTS

An example of the time-profiles obtained from each plasma discharge is shown in figure 2. The discharges showed clear periods of stability, particularly with regard to U_{loop}, and these stable regions determined the windows for the calculation of the average values $\langle B_T \rangle$, $\langle I_P \rangle$ and $\langle T_e \rangle$ for each shot. The dependence of $\langle T_e \rangle$ on $\langle B_T \rangle$ and $\langle I_P \rangle$ is shown in the contour plot figure 3. A similar contour plot was also produced to map the dependence of the shot duration, Δt on U_{BT} and U_{CD}. This plot is shown in figure 4, with the discharge that acheived the highest $\langle T_e \rangle$ also marked. A further graph, figure 6, was also produced to visualise the degree to which the average temperature acheived in a discharge depended on its duration, and shows a linear positive correlation. To support conclusions related to the input capacitor charging

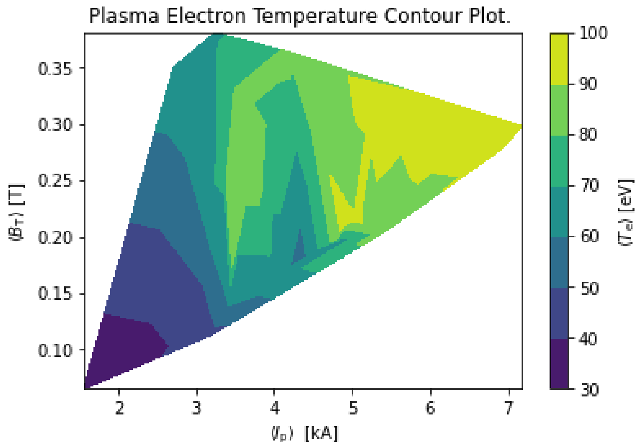

FIG. 3: Contour plot of $\langle T_e \rangle$, as a function of $\langle B_T \rangle$ and $\langle I_P \rangle$ across all 35 discharges.

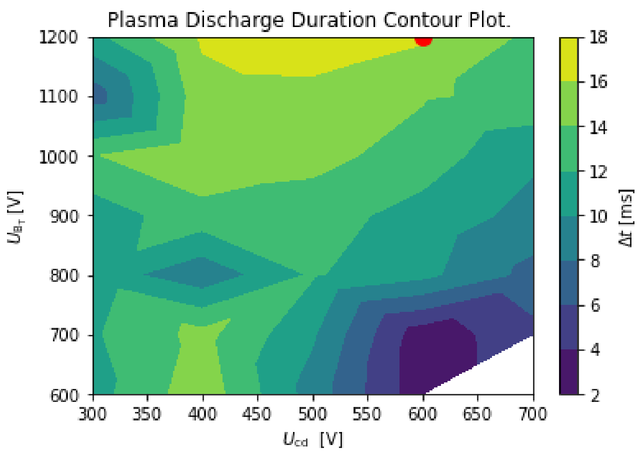

FIG. 4: Contour plot of plasma discharge duration Δt as a function of (U_{BT}) and (U_{CD}). The red marker at (600,1200) shows the shot which acheived the highest average electron temperature $\langle T_e \rangle$.

voltages U_{CD} and U_{BT}, two calibration plots were also produced: the first of the maximum value of B_T in each discharge versus U_{BT} for each discharge at $U_{CD} = 400$V, and the second of the maximum value of I_P in each discharge versus U_{CD} for each discharge at $U_{BT} = 1200$V (figure 5). These simply confirm the linear proportionailty of B_T and I_P to U_{BT} and U_{CD} respectively over the vast majority of the scanned range of capacitor voltages, except for a plateau in I_P at the highest current drive voltages.

VI. DISCUSSION

Figure 3 shows that the average electron temperature acheived during a shot increases when both $\langle B_T \rangle$ and $\langle I_P \rangle$ are increased concurrently, but does not increase as much if either variable is increased without a comensurate increase in the other. The maximum of average electron temperature is hence observed in the top-right part of the plot. This result fits well with the theoretical prediction that a stronger confining field reduces the loss of high energy electrons from the plasma, and that a sufficiently high poloidal magnetic field component is also required to stabilise the plasma against outward major-radial drift. Higher magnetic field strength leads to the trapping of electrons up to a higher maximum velocity, hence enabling the electron velocity distribution to attain a higher temperature. Since the source of electron heating is ohmic, the higher I_P the higher the heating power and the higher the electron temperature that can be reached within a given discharge duration.

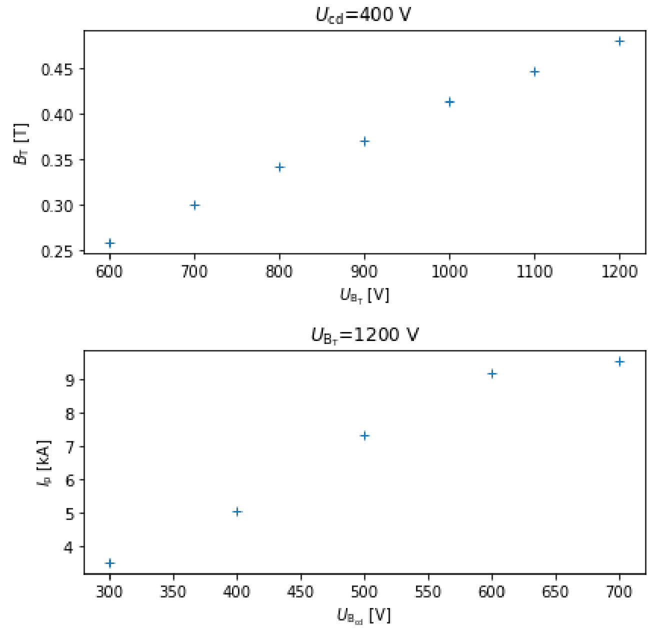

FIG. 5: Top: Calibration plot of the measured B_T, versus U_{BT}, at a fixed value of U_{CD} (400V). Bottom: Calibration plot of the measured I_P, versus U_{CD}, for a fixed value of U_{BT} (1200V).

The 'triangular' nature of figure 3 is an interesting result. The white spaces bordering both axes and expanding at both high current and high magnetic field correspond to areas for which no data points were obtained in this 'mean parameter' space. These might suggest that creation of B_T and I_P are in fact coupled processes, hence attempting to vary $\langle B_T \rangle$ whilst keeping $\langle I_P \rangle$ fixed cannot be acheived by simply varying U_{BT} and keeping U_{CD} fixed. The phenomenon of the 'bootstrap current'[6] may contribute to the increase in $\langle I_P \rangle$ when $\langle B_T \rangle$ is varied at fixed U_{CD}, but there is no physical equivalent for the increase in B_T with I_P at fixed U_{BT}. The triangular appearance is therefore most probably an artefact of the windowed avergaing technique used to calculate mean values.

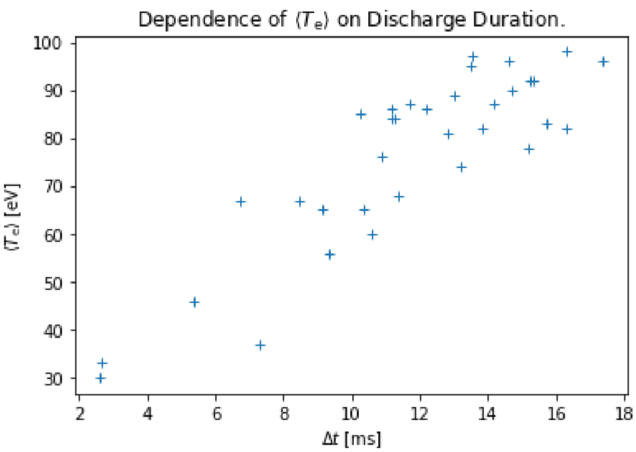

FIG. 6: Variation of $\langle T_e \rangle$) with discharge duration (Δt).

Figure 4 was produced to investigate the dependence of the discharge duration (Δt) on U_{BT} and U_{CD}. The discharge duration provides a good measure of the overall stability of a particular plasma. Figure 4 shows that plasma stability is compromised at the extremes of both high U_{BT} coupled with low U_{CD}, and vice versa. The maximum of the contour plot occurs at $U_{BT} = 1200$V, $U_{CD} \approx 500$V, suggesting that this combination of the discharge voltages produces an especially stable combination of toroidal and poloidal magnetic fields (with a high saftey factor q, whilst remaining stable against secular drifts). By contrast, it can be clearly seen that the discharge duration falls off toward the lower right corner of the plot, with the white space around $U_{CD} = 700$V, $U_{BT} = 600$V corresponding to the discharge which failed to breakdown the gas in the tokamak. This is possibly due to these discharges resulting in low values of the safety factor q. In the large aspect-ratio limit for a tokamak with circular cross section (such as GOLEM), the value of q on a particular flux surface is defined approximately according to the following equation.

$$q \approx \frac{r}{R_0} \frac{B_T}{B_\theta} \tag{2}$$

Where r is the minor-radius of the flux surface, R_0 is the major radius of the tokamak and B_θ is the poloidal magnetic field strength on the flux surface. In the tokamak, the theory of magneto-hydrodynamic (MHD) stability states that, in general, the higher the value of q, the more stable the tokamak plasma[6]. This theory could explain the observed short duration of the discharges at high I_P but low B_T; they are MHD unstable due to their low values of q (since $B_\theta \propto I_P$).

Figure 6 also shows that the value of $\langle T_e \rangle$ acheived during a given discharge was positively correlated with the discharge's duration. This suggests that the same conditions that produce a stable plasma also enable that plasma to attain a higher temperature, an encouraging result for the prospects of MCF, if applicable to tokamaks generally. However, it is likely that this figure is actually simply revealing the correlation between I_P and T_e over time, as shown previously in figure 2. These GOLEM discharges did not reach the 'flat-top' conditions obtained in other, larger tokamaks[4], where I_P and T_e stabilise to relatively constant values for large periods of a discharge, and instead I_P and T_e both increase continuously until termination. T_e increases with I_P due to ohmic heating, the only source of heating in GOLEM. Hence, the longer the duration of the discharge, the higher the value of $\langle T_e \rangle$. Since tokamak power plant discharges are expected to reach 'flat-top' conditions quickly and maintain this state for the vast majority of their duration, the result shown in figure 6 is not as encouraging as it might initially appear.

VII. CONCLUSION

The variation of $\langle T_e \rangle$ with $\langle B_T \rangle$, $\langle I_P \rangle$ and discharge duration Δt has been explored. It has been found that $\langle T_e \rangle$ increases when both $\langle B_T \rangle$ and $\langle I_P \rangle$ are increased simultaneously, but falls in unbalanced extremes of either variable. An explanation in terms of MHD stability has been proposed. A positive correlation between $\langle T_e \rangle$ and Δt has been observed, and this has been related to the ohmic nature of the plasma heating on GOLEM, as well as the lack of a 'flat-top' in the discharge profiles. Regions of the ($\langle B_T \rangle$, $\langle I_P \rangle$) parameter space that were not explored in this work would be of interest to examine in a future discharge campaign, but this would require correction for the coupled generation of B_T and I_P also detected in this work.

REFERENCES

[1] Francis F Chen **andothers**. *Introduction to plasma physics and controlled fusion.* **volume** 1. Springer, 1984.

[2] Robert S Cohen, Lyman Spitzer Jr **and** Paul McR Routly. "The electrical conductivity of an ionized gas". **in**: *Physical Review* 80.2 (1950), **page** 230.

[3] O Grover **andothers**. "Remote operation of the GOLEM tokamak for Fusion Education". **in**: *Fusion Engineering and Design* 112 (2016), **pages** 1038–1044.

[4] SH Kim **andothers**. "Full tokamak discharge simulation of ITER by combining DINA-CH and CRONOS". **in**: *Plasma Physics and Controlled Fusion* 51.10 (2009), **page** 105007.

[5] Lyman Spitzer **and** Richard Härm. "Transport Phenomena in a Completely Ionized Gas". **in**: *Phys. Rev.* 89 (5 **march** 1953), **pages** 977–981. DOI: `10.1103/PhysRev.89.977`. URL: `https://link.aps.org/doi/10.1103/PhysRev.89.977`.

[6] John Wesson **and** David J Campbell. *Tokamaks.* **volume** 149. Oxford university press, 2011.